NEURAL REGENERATION RESEARCH
December 2016, Volume 11, Issue 12
www.nrronline.org

RESEARCH ARTICLE

Cortical regulation of striatal projection neurons and interneurons in a Parkinson's disease rat model

Jia-jia Wu[1,2], Si Chen[1], Li-si Ouyang[1], Yu Jia[1], Bing-bing Liu[3], Shu-hua Mu[4], Yu-xin Ma[1], Wei-ping Wang[1], Jia-you Wei[1], You-lan Li[1], Zhi Chen[1], Wan-long Lei[1,*]

1 Department of Anatomy, Zhongshan School of Medicine, Sun Yat-sen University, Guangzhou, Guangdong Province, China
2 Periodical Center, the Third Affiliated Hospital, Sun Yat-sen University, Guangzhou, Guangdong Province, China
3 Department of Anesthesiology, Guangdong No. 2 Provincial People's Hospital, Guangdong Provincial Emergency Hospital, Guangzhou, Guangdong Province, China
4 Key Laboratory of Optoelectronic Devices and Systems of Ministry of Education and Guangdong Province, College of Optoelectronic Engineering, Shenzhen University, Shenzhen, Guangdong Province, China

How to cite this article: *Wu JJ, Chen S, Ouyang LS, Jia Y, Liu BB, Mu SH, Ma YX, Wang WP, Wei JY, Li YL, Chen Z, Lei WL (2016) Cortical regulation of striatal projection neurons and interneurons in a Parkinson's disease rat model. Neural Regen Res 11(12):1969-1975.*

Funding: *This study was supported by the National Natural Science Foundation of China, No. 81471288.*

Graphical Abstract

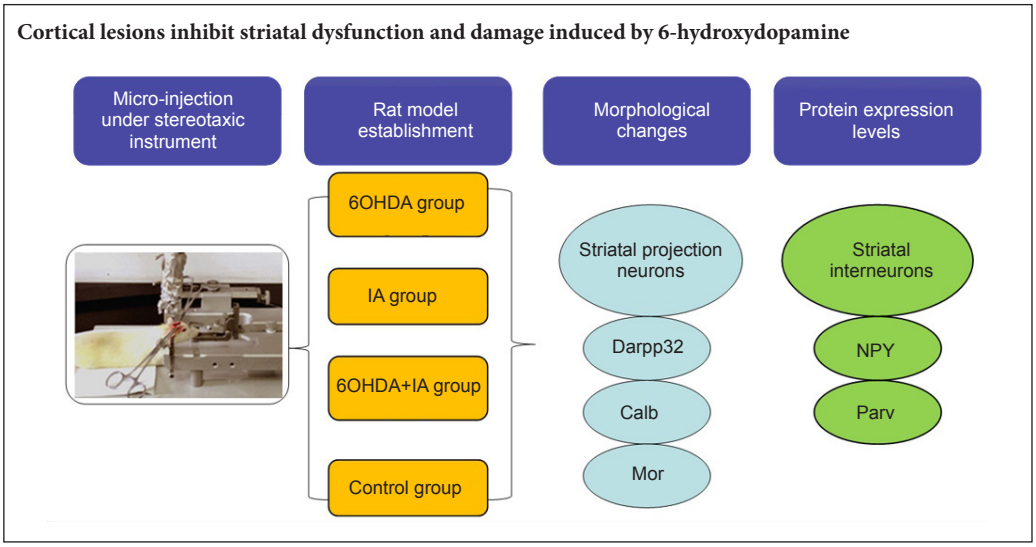

Correspondence to:
Wan-long Lei, Ph.D.,
leiwl@mail.sysu.edu.cn.

orcid:
0000-0002-0555-7428
(Wan-long Lei)

doi: *10.4103/1673-5374.197140*

Accepted: *2016-11-29*

Abstract

Striatal neurons can be either projection neurons or interneurons, with each type exhibiting distinct susceptibility to various types of brain damage. In this study, 6-hydroxydopamine was injected into the right medial forebrain bundle to induce dopamine depletion, and/or ibotenic acid was injected into the M1 cortex to induce motor cortex lesions. Immunohistochemistry and western blot assay showed that dopaminergic depletion results in significant loss of striatal projection neurons marked by dopamine- and cyclic adenosine monophosphate-regulated phosphoprotein, molecular weight 32 kDa, calbindin, and μ-opioid receptor, while cortical lesions reversed these pathological changes. After dopaminergic deletion, the number of neuropeptide Y-positive striatal interneurons markedly increased, which was also inhibited by cortical lesioning. No noticeable change in the number of parvalbumin-positive interneurons was found in 6-hydroxydopamine-treated rats. Striatal projection neurons and interneurons show different susceptibility to dopaminergic depletion. Further, cortical lesions inhibit striatal dysfunction and damage induced by 6-hydroxydopamine, which provides a new possibility for clinical treatment of Parkinson's disease.

Key Words: *nerve regeneration; motor cortex lesions; dopaminergic neurons; GABAergic neurons; Darpp32; calbindin; μ-opioid receptor; neuropeptide Y; parvalbumin; neural regeneration*

Introduction

Parkinson's disease (PD) is a common neurodegenerative disease caused by dopaminergic (DA) neuronal degeneration/loss in the midbrain substantia nigra compacta (Wood, 2010; Morley and Duda, 2012). Pathomechanisms of PD include genetic mutations, the environment, oxidative stress, calcium dyshomeostasis, excitotoxicity, mitochondrial dysfunction, cell apoptosis, overexpression of related proteins, and immunological factors (Colosimo et al., 2003; Perier et al., 2011; Müller et al., 2013). Indeed, loss of midbrain DA neurons is only the initial trigger for complex pathological changes (Wirdefeldt et al., 2011). Consequently, loss of DA neurons in the substantia nigra results in striatal DA neurotransmitter depletion, and causes morphological and functional changes in the corpus striatum (Zhou et al., 2014; Xiao, 2015; Jimenez-Shahed, 2016).

Striatal neurons include projection neurons (approximately 95% in rodents) and interneurons (5% in rodents) (Gerfen and Surmeier, 2011). Projection neurons are γ-aminobutyric acid (GABA)-ergic inhibitory neurons, which can be specifically marked by dopamine- and cAMP-regulated phosphoprotein, molecular weight 32 kDa (Darpp32), calbindin (Calb), and μ-opioid receptor (Mor) (Reiner et al., 1998; Dopeso-Reyes et al., 2014; Fu et al., 2016). Moreover, studies have confirmed four types of striatal interneurons: parvalbumin $(Parv)^+$, calretinin $(Cr)^+$, neuropeptide Y/somatostatin/neuronal nitric oxide synthase $(NPY/SS/nNOS)^+$, and choline acetyltransferase $(CHAT)^+$ (Kawaguchi, 1997; Gittis and Kreitzer, 2012). In addition, these different types of striatal neurons exhibit distinct susceptibility to various types of brain damage (Mallet et al., 2006; Planert et al., 2010). Vulnerability of projection neurons and resistance of interneurons are widely reported in cerebral ischemia and Huntington's disease models induced by 3-nitropropionic acid or quinolinic acid (Ma et al., 2013; Feng et al., 2014; Mu et al., 2014). Although the pathological mechanism of striatal projection neuron injury following DA depletion induced by 6-hydroxydopamine (6OHDA) remains unclear, our previous studies have shown that DA depletion results in sensorimotor and cognitive dysfunction in experimental rats, with a characteristic hyperplastic reaction of striatal interneurons (Jia et al., 2014; Ma et al., 2014).

Striatal projection neurons receive excitatory glutamatergic inputs from the cortex and thalamus, and DA input from the mesencephalon, which thereby maintains a dynamic balance in their morphology and function (Ingham et al., 1998; Gerfen, 2006; Lovinger, 2010; Macpherson et al., 2014). Therefore, degeneration of DA neurons leads to disruption of the balance between excitatory and inhibitory inputs in striatal projection neurons, as well as abnormal activity of direct and indirect pathway neurons (Do et al., 2013). Further, striatal DA depletion decreases the number of dendritic spines on projection neurons, which may reflect removal of tonic DA inhibitory control over corticostriatal glutamatergic drive, resulting in increased glutamatergic release, and culminating in spine loss (Garcia et al., 2010). To determine if changes in projection neurons and interneurons require glutamatergic release (and hence if cortical lesions mitigate damage by suppressing glutamatergic release), we used a DA depletion model (substantia nigra of the midbrain), glutamatergic depletion model (cortex), and DA + glutamatergic depletion model to investigate histopathological and protein changes in projection neurons and interneurons. Our aim was to provide comprehensive evidence on the pathological mechanisms of PD and the effect of cortical lesions in a PD model.

Materials and Methods

Animals

In total, 40 specific-pathogen-free adult male Sprague-Dawley rats (Sun Yat-sen University, China; SCXK2016-0029) weighing 250–300 g were group housed under a 12-hour light/dark cycle with access to food and water. All animal experiments were performed with the approval of the Animal Care and Use Committee of Sun Yat-sen University. Rats were randomly divided into four groups: 6OHDA (n = 10), ibotenic acid (IA) (n = 10), 6OHDA + IA (n = 10), and control (n = 10).

Rat treatment

The methods used in the present study have been previously described in detail (Jia et al., 2014; Ma et al., 2014). Briefly, rats in the 6OHDA group received a unilateral injection of 6OHDA (Sigma, St. Louis, MO, USA) into the right median forebrain bundle at a final dosage of 5.4 μg (Jia et al., 2014; Ma et al., 2014). Rats were then anesthetized with chloral hydrate (150 mg/kg) and placed onto a Kopf stereotaxic instrument (Stoelting, Wood Dale, IL, USA). Two skull areas were exposed (coordinates: lateral = −1.8 mm, anterior = −4.2 mm, vertical = −8.1 mm; and lateral = −1.4 mm, anterior = −4.5 mm, and vertical = −8.0 mm). Next, 6OHDA (3 μg/μL; 6OHDA dissolved in 0.9% saline containing 0.01% ascorbic acid as an antioxidant) was injected using a 10 μL syringe (Hamilton, Reno, NV, USA). With rats in the IA group, motor cortex lesions were produced by unilaterally injecting a 1.0 μL volume of 45 nM IA (Sigma) into the M1 cortex (lateral = +1.7 mm, anterior = +2.2 mm, and vertical = –1.7 mm) at a rate of 200 nL/min the (Garcia et al., 2010). Rats in the 6OHDA + IA group received unilateral injection of both 6OHDA and IA using the same method.

At 2 and 4 weeks after 6OHDA lesion, rats were assessed by apomorphine-induced rotation. Rats were subcutaneously injected with apomorphine (Tocris, Bristol, UK) at a dose of 0.25 mg/kg. Next, the number of 360° contralateral rotations was counted for 30 minutes. Only rats with significant contralateral rotations (> 7 cycles per minute or total cycles > 210) were included (Jia et al., 2014; Ma et al., 2014). All rats were killed at 28 days after surgery and further examined.

Immunohistochemistry

Rats were anesthetized with chloral hydrate (0.4 g/kg) (Aoxin, Yangzhou, Jiangsu Province, China), and then transcardially perfused with 0.9% saline, followed by 4% paraformaldehyde (400 mL) in 0.01 M phosphate buffer (pH 7.4, 4°C). Brains were quickly removed, immersed in the same fixative overnight at 4°C, then transferred into graded sucrose and subsequently frozen. Sections (each of 40 μm) containing the

corpus striatum were cut using a cryoultramicrotome, and then pretreated in 0.3% H_2O_2 in 0.01 M phosphate buffer (pH 7.4) for 30 minutes. Sections were washed three times in 0.01 M phosphate buffer (pH 7.4) for 5 minutes before antibody incubation.

Sections were incubated with the following primary antibodies for 36 hours at 4°C: rabbit anti-Darpp32 (1:250; Cell Signaling, Danvers, MA, USA), rabbit anti-Mor (1:1,000; Chemicon, Rolling Meadows, IL, USA), mouse anti-Calb (1:1,000; Sigma), rabbit anti-NPY (1:3,000; Abcam, Cambridge, UK), and mouse anti-Parv (1:1,000; Sigma). Afterwards, sections were incubated with the following secondary antibodies for 3 hours at room temperature: goat anti-rabbit IgG or goat anti-mouse IgG (both 1:200; Sigma), and then washed and incubated with homologous peroxidase anti-peroxidase complex (1:100; Sigma) at room temperature for 2 hours. Standard avidin-biotin binding was detected using 3,3′-diaminobenzidine (0.05% in 0.01 M phosphate buffer, pH 7.4; Sigma) for 2–8 minutes. Unequivocally positive neurons were counted using ImageJ software (National Institutes of Health, Bethesda, MD, USA). The sections were selected from every fifth section of the brain containing the striatum (three sections per animal for each staining method). Average positive area (%, expressed as positive expression percentage) and number of positive cells per mm^2 were calculated. The cell counts of $Darpp32^+$, $Parv^+$ and NPY^+ neurons were determined as follows: each section was first viewed at 100× magnification with a reticule (0.1 mm × 0.1 mm) in one eye piece to observe the whole striatum, and then the reticule was randomly moved into five nonoverlapping regions (0.01 mm^2 for each) within striatum, and the cell count was performed within the reticule field at 400× magnification. In addition, the positive area of Mor^+ and $Calb^+$ neurons was quantified by ImageJ software.

Western blot assay

After deep anesthesia with chloral hydrate (0.5 g/kg), rats were killed by decapitation and the striatum extracted and homogenized. Next, 30 μg of total protein from each sample was separated on 10% sodium dodecyl sulfate-polyacrylamide gel electrophoresis gels and transferred to polyvinylidene fluoride membrane. After blocking with 5% nonfat dry milk for 2 hours at room temperature, membranes were incubated overnight at 4°C with primary antibodies: rabbit anti-Darpp32 (1:250; Cell Signaling), rabbit anti-NPY (1:3,000; Abcam), mouse anti-Parv (1:1,000; Sigma), and rabbit anti-β-actin (1:2,000; Millipore, Billerica, MA, USA). Afterwards, membranes were incubated with horseradish peroxidase conjugated anti-rabbit and anti-mouse secondary antibodies (1:3,000; Millipore) for 2 hours at room temperature. Blots were visualized using an enhanced chemiluminescence system (GE, Fairfield, CT, USA), as previously described, and quantified by optical density using ImageJ software.

Statistical analysis

SPSS 19.0 software (IBM, Armonk, New York, USA) was used for all statistical analyses. All experimental data are expressed as the mean ± SD. Comparisons among groups were examined by one-way analysis of variance and Student's *t*-test. $P < 0.05$ was considered statistically significant.

Results

Effect of cortical lesions on striatal projection neuron morphology

Using Darpp32 as a marker of striatal projection neurons, immunohistochemical staining showed that Darpp32 neurons were of similar median size and uniformly distributed throughout the striatum (**Figure 1**). Statistical analysis showed lower neuronal $Darpp32^+$ immunoreactivity in the 6OHDA group compared with the control and IA groups. In contrast, neuronal $Darpp32^+$ immunoreactivity was higher in the 6OHDA + IA group compared with the 6OHDA group (all $P < 0.05$; **Figure 2D**).

Immunohistochemical staining of Mor and Calb, which are also specific labels for projection neurons, showed that Mor^+ neurons were expressed as a plaque area with a clear boundary. Moreover, $Calb^+$ neurons were expressed as a large positive area with a small area of light staining (**Figure 3**). Statistical analysis showed significantly less Mor immunoreactivity in the 6OHDA group compared with the control and IA groups, yet higher immunoreactivity in the 6OHDA + IA group compared with the 6OHDA group (all $P < 0.05$; **Figure 2C**). Calb immunoreactivity was also less in the 6OHDA group compared with the other groups (all $P < 0.05$; **Figure 2C**).

Effect of cortical lesions on striatal interneuron morphology

Immunohistochemical staining showed a sparse distribution of median sized NPY^+ and $Parv^+$ neurons (**Figure 4**). Statistical analysis showed higher neuronal NPY^+ immunoreactivity in the 6OHDA group compared with the control and IA groups, but lower immunoreactivity in the 6OHDA + IA group compared with the 6OHDA group (all $P < 0.05$; **Figure 2D**). Neuronal $Parv^+$ immunoreactivity was not significantly different among the four groups (all $P > 0.05$; **Figure 2D**).

Effect of cortical lesions on protein expression levels in striatal projection neurons and interneurons

Western blot assays showed significantly lower expression levels of striatal Darpp32 protein in the 6OHDA group compared with the control and IA groups, but higher levels in the 6OHDA + IA group compared with the 6OHDA group (all $P < 0.05$; **Figure 2A**, **B**). Expression levels of striatal NPY protein were significantly higher in the 6OHDA group compared with the control group ($P < 0.05$; **Figure 2A**, **B**), while no significant difference was found between the IA and 6OHDA + IA groups (both $P > 0.05$; **Figure 2A–B**). There was no significant difference in Parv protein expression levels among the four groups (all $P > 0.05$; **Figure 2A**, **B**).

Discussion

The striatum is the main component of the basal ganglia, and

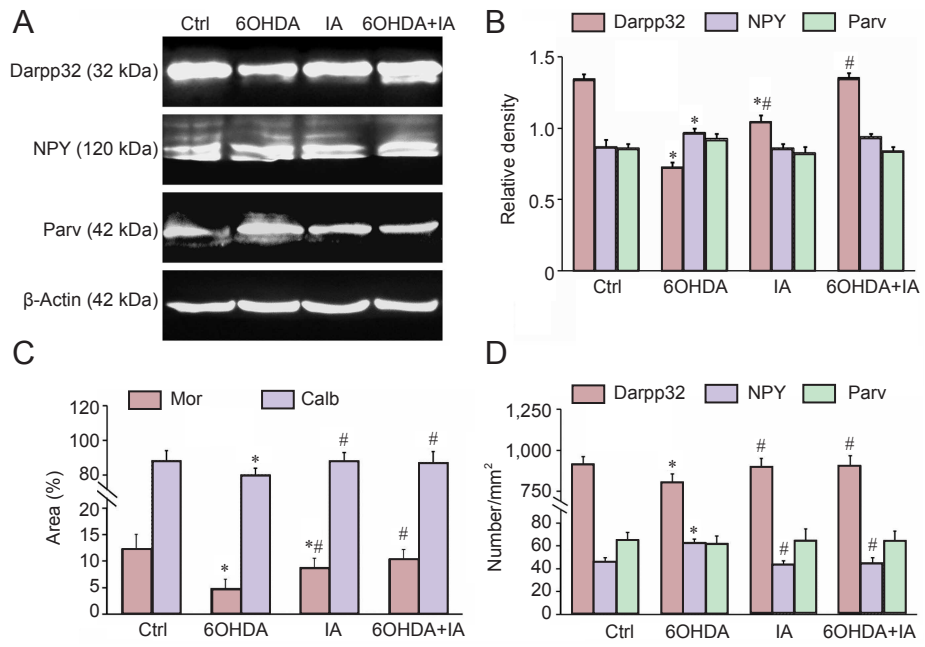

Figure 2 Effect of cortical lesions on levels of striatal Darpp32/NPY/Parv proteins in a Parkinson's disease rat model.

(A) Western blot assay results showing Darpp32, NPY, and Parv protein expression levels in the striatum of all four groups. (B) Western blot quantitation results are represented as the optical density ratio of the target protein to β-actin. (C) Area of Mor$^+$ and Calb$^+$ projection neurons in the striatum. (D) Number of Darpp32$^+$ projection neurons and NPY$^+$ and Parv$^+$ interneurons in the striatum. All data are expressed as the mean ± SD. Comparisons among groups were examined by one-way analysis of variance and Student's *t*-test. **P* < 0.05, *vs.* Ctrl group; #*P* < 0.05, *vs.* 6OHDA group. The experiment was performed five times. Darpp32: Dopamine- and cAMP-regulated phosphoprotein, molecular weight 32 kDa; NPY: neuropeptide Y; Parv: parvalbumin; Mor: μ-opioid receptor; Calb: calbindin; Ctrl: control; 6OHDA: 6-hydroxydopamine; IA: ibotenic acid.

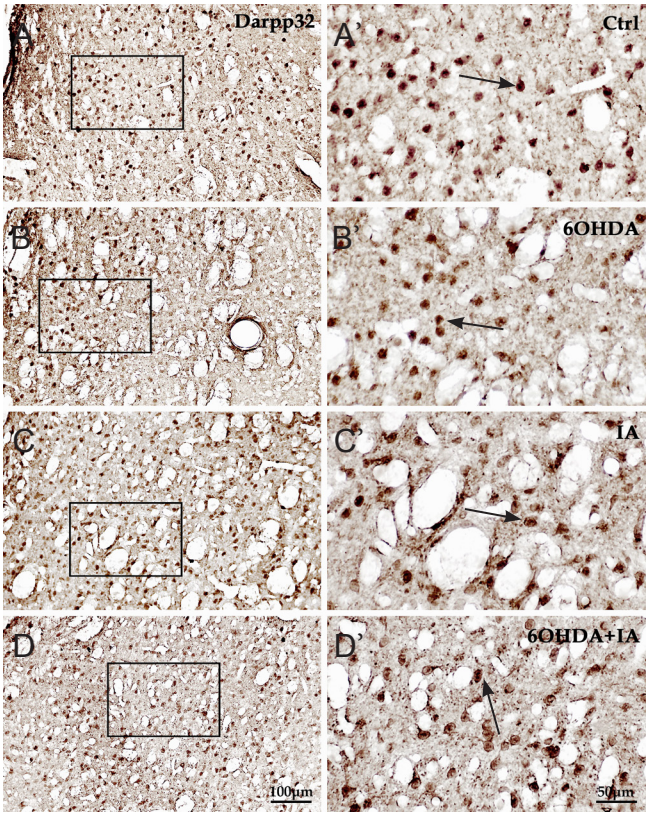

Figure 1 Effect of cortical lesions on Darpp32$^+$ projection neurons in the striatum of a Parkinson's disease rat model.

(A–D) Low power light microscopic images of immuohistochemical staining. (A'–D') High magnification of A–D: Darpp32$^+$ neuronal number decreased in the 6OHDA group compared with the control group. In contrast, Darpp32$^+$ neuronal number increased significantly in the 6OHDA + IA group. Scale bars: 100 μm in A–D, 50 μm in A'–D'. Darpp32: Dopamine- and cAMP-regulated phosphoprotein, molecular weight 32 kDa; Ctrl: control; 6OHDA: 6-hydroxydopamine; IA: ibotenic acid. Arrows indicate Darpp32$^+$ projection neurons.

has a complex cell structure and neurochemical phenotype. Striatal neurons are divided into projection neurons and interneurons according to cellular morphology and function (Flores-Barrera et al., 2010). In mammals, DARPP32 is a D1-receptor associated signaling protein found in striatal projection neurons, including both substance P-containing-positive neurons and enkephalinergic projection neurons (Reiner et al., 1998). The striatum can also be divided into patch (striosome) and matrix compartments based on differential connectivity and expression of neuropeptides and receptors (Gerfen et al., 1985; Graybiel, 1990; Crittenden and Graybiel, 2011). The patch compartment is thought to be a limbic channel that runs through the striatum, and receives input from the prelimbic cortex and amygdala. Alternatively, the matrix compartment is considered to be a motor channel that traverses the striatum, and it receives inputs from sensorimotor and associative forebrain regions (Gerfen, 1984; Ragsdale and Graybiel, 1988; McDonald, 1992). The striatum also contains a small amount of interneurons including Parv$^+$, NPY$^+$, Cr$^+$, and Chat$^+$ neurons (Galarreta and Hestrin, 2001). Striatal projection neurons in direct and indirect pathways have opposite effects in regulating movement function of the cerebral cortex, while interneurons function in regulation of projection neurons *via* GABA microcircuits (Ballion et al., 2008; Planert et al., 2010).

Striatal DA neurons are lost during the pathological changes of PD. However, different types of striatal neurons exhibit different degrees of damage in PD. Various striatal neurons show different sensitivity in the pathological process of PD (Jia et al., 2014; Ma et al., 2014). In the striatum, medium spiny GABA projection neurons are damaged first, especially indirect pathway neurons (D2$^+$) (Day et al., 2008; Tozzi et al., 2011; Kim et al., 2013). Conversely, striatal interneurons show strong resistance to pathological damage. Our

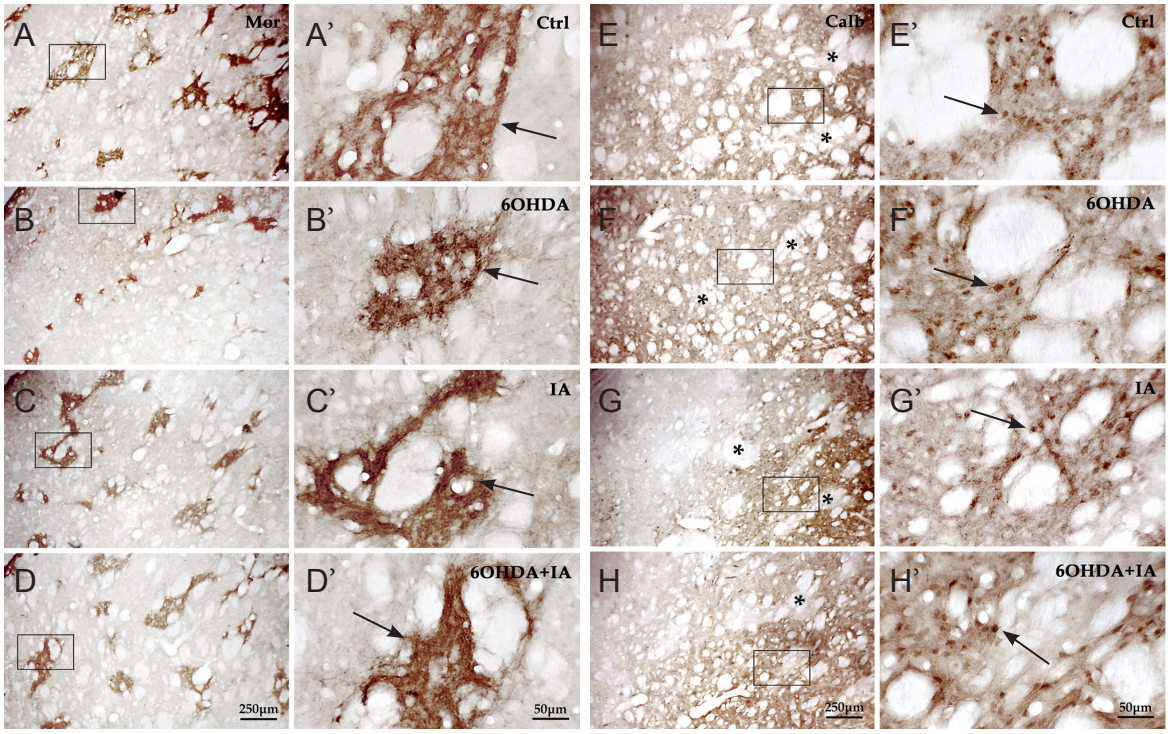

Figure 3 Effect of cortical lesions on Mor$^+$ and Calb$^+$ projection neurons in the striatum of a Parkinson's disease rat model.
(A–D) Low power light microscopic images of immuohistochemical staining for Mor$^+$ projection neurons. (A'–D') High magnification views. Arrows indicate Mor$^+$ projection neurons. Mor$^+$ neuronal area decreased in the 6OHDA group compared with the control group. However, Mor$^+$ neuronal area increased significantly in the 6OHDA + IA group. (E–H) Simultaneous visualization of Calb$^+$ projection neurons in all four groups at low magnification. E'–H' are from the corresponding images E–H. Arrows indicate Calb$^+$ projection neurons. Minimal hyperchromatism areas marked by * were observed in images E–H, which represent Patch intermediate zones. Scale bars: 250 μm in A–H, 50 μm in A'–H'. Mor: μ-opioid receptor; Calb: calbindin; Ctrl: control; 6OHDA: 6-hydroxydopamine; IA: ibotenic acid.

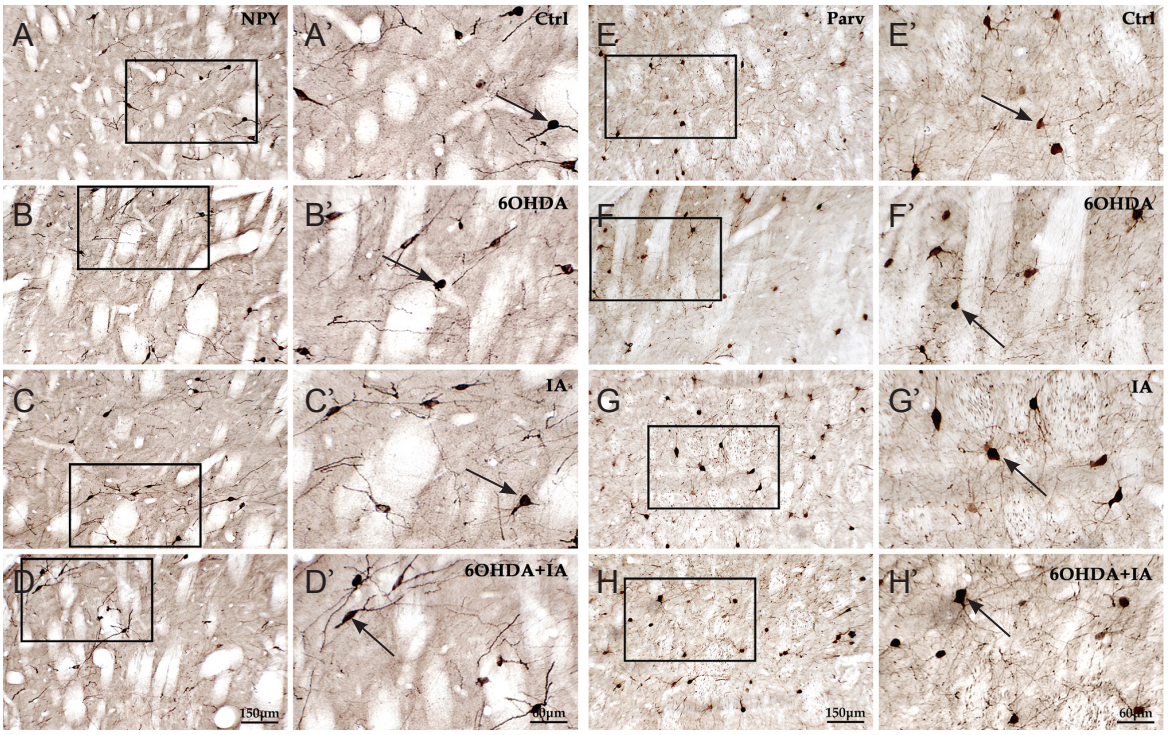

Figure 4 Effect of cortical lesions on NPY$^+$ and Parv$^+$ interneurons in the striatum of a Parkinson's disease rat model.
A–D and A'–D' show the distribution pattern and morphology of striatal NPY$^+$ interneurons by immunohistochemical staining. A–A', B–B', C–C', and D–D' show NPY$^+$ interneurons (arrows) in Ctrl, 6OHDA, IA, and 6OHDA + IA groups, respectively. E–H and E'–H': distribution pattern and morphology of striatal Parv$^+$ interneurons. E–E', F–F', G–G', and H–H': Parv$^+$ interneurons (arrows) in Ctrl, 6OHDA, IA, and 6OHDA + IA groups, respectively. Scale bars: 150 μm in A–H, 60 μm in A'–H'. NPY: Neuropeptide Y; Parv: parvalbumin; Ctrl: control; 6OHDA: 6-hydroxydopamine; IA: ibotenic acid.

previous studies confirmed that four interneuron types show intense proliferative changes in middle cerebral artery occlusion and quinolinic acid models, as well as characteristic changes during 6OHDA-induced DA depletion (Ma et al., 2013, 2014; Feng et al., 2014; Mu et al., 2014). In the present study, we used immunohistochemistry and western blot assays to examine the damage to striatal projection neurons and interneurons in a PD model. Our results show that the number of Darpp32$^+$ projection neurons and areas of Mor$^+$ and Calb$^+$ projection neurons decreased significantly after DA depletion induced by 6OHDA. However, reduction of Darpp32, Calb, and Mor was not observed in the 6OHDA + IA group. Protein expression levels of Darpp 32 also exhibited the same trend as our immunohistochemical results. Thus, our study confirms that projection neurons are sensitive to damage following DA depletion, while cortical lesions reverse the reaction of projection neurons.

Our previous studies confirmed that striatal interneurons are tolerant to pathological lesions of PD, but do not completely escape from damage. In the present study, we chose two characteristic interneuron markers, NPY and Parv, to observe neuronal changes in morphology and protein levels. In our PD model, NPY$^+$ interneurons showed a proliferative reaction, with increased number and protein levels, consistent with our previous study (Ma et al., 2014). The significance of this phenomenon is still unclear. It may reflect reactive hyperplasia to DA depletion injury or a feedback response to loss of projection neurons (e.g., projection neurons may inhibit the interneuron reaction). All of these possibilities require further studies. However, increased number and protein levels of NPY$^+$ interneurons were not detected in our PD model after cortical lesions. Moreover, no significant change in Parv$^+$ interneurons was observed in any group. This result also shows that cortical lesions inhibit striatal dysfunction and injury induced by 6OHDA. The metabotropic glutamate (mGluR) 2/3 receptor agonist, LY379268, is a preferential agonist at mGluR2/3 receptors (Schoepp et al., 1999; Imre, 2007). The effect of LY379268 on PD-related motor deficits was confirmed by suppressing corticostriatal glutamate release (Murray et al., 2002; Garcia et al., 2010), which will be our future research aim.

In summary, our study is the first to compare striatal projection neurons and interneurons following cortical lesions of DA depletion. Our findings demonstrate that 6OHDA-induced DA depletion causes reduced Darpp32, Mor, and Calb immunohistochemical staining (number and positive area), and reduces protein levels for striatal projection neurons. Meanwhile, cortical lesions reversed these pathological changes. 6OHDA-induced DA depletion results in increased number and protein levels of NPY interneurons, which is also inhibited by cortical lesions. No morphological or protein changes were observed in Parv interneurons after 6OHDA-induced DA depletion and cortical lesions. Taken together, striatal projection neurons and interneurons exhibit different susceptibility to DA depletion. While cortical lesions inhibit striatal dysfunction and damage induced by 6OHDA, providing a new possibility for clinical treatment of PD.

Author contributions: *WLL participated in study design. JJW and SC participated in literature research. JJW, YJ and WPW performed experimental studies. JJW, LSO and BBL conducted data acquisition/analysis. JJW and SHM participated in statistical analysis. JJW, SC and YXM prepared the paper. JJW, JYW, YLL and ZC edited the paper. All authors participated in manuscript revision/review, and approved the final version of the paper.*
Conflicts of interest: *None declared.*
Plagiarism check: *This paper was screened twice using CrossCheck to verify originality before publication.*
Peer review: *This paper was double-blinded and stringently reviewed by international expert reviewers.*

References

Ballion B, Mallet N, Bézard E, Lanciego JL, Gonon F (2008) Intratelencephalic corticostriatal neurons equally excite striatonigral and striatopallidal neurons and their discharge activity is selectively reduced in experimental parkinsonism. Eur J Neurosci 27:2313-2321.

Colosimo C, Hughes A, Kilford L, Lees A (2003) Lewy body cortical involvement may not always predict dementia in Parkinson's disease. J Neurol Neurosurg Psychiatry 74:852-856.

Crittenden JR, Graybiel AM (2011) Basal Ganglia disorders associated with imbalances in the striatal striosome and matrix compartments. Front Neuroanat 5:59.

Day M, Wokosin D, Plotkin JL, Tian X, Surmeier DJ (2008) Differential excitability and modulation of striatal medium spiny neuron dendrites. J Neurosci 28:11603-11614.

Do J, Kim JI, Bakes J, Lee K, Kaang BK (2013) Functional roles of neurotransmitters and neuromodulators in the dorsal striatum. Learn Mem 20:21-28.

Dopeso-Reyes IG, Rico AJ, Roda E, Sierra S, Pignataro D, Lanz M, Sucunza D, Chang-Azancot L, Lanciego JL (2014) Calbindin content and differential vulnerability of midbrain efferent dopaminergic neurons in macaques. Front Neuroanat 8:146.

Feng Q, Ma Y, Mu S, Wu J, Chen S, OuYang L, Lei W (2014) Specific reactions of different striatal neuron types in morphology induced by quinolinic acid in rats. PLoS One 9:e91512.

Flores-Barrera E, Vizcarra-Chacón BJ, Tapia D, Bargas J, Galarraga E (2010) Different corticostriatal integration in spiny projection neurons from direct and indirect pathways. Front Syst Neurosci 4:15.

Fu R, Chen X, Zuo W, Li J, Kang S, Zhou L-H, Siegel A, Bekker A, Ye J-H (2016) Ablation of μ opioid receptor-expressing GABA neurons in rostromedial tegmental nucleus increases ethanol consumption and regulates ethanol-related behaviors. Neuropharmacology 107:58-67.

Galarreta M, Hestrin S (2001) Spike transmission and synchrony detection in networks of GABAergic interneurons. Science 292:2295-2299.

Garcia BG, Neely MD, Deutch AY (2010) Cortical regulation of striatal medium spiny neuron dendritic remodeling in parkinsonism: modulation of glutamate release reverses dopamine depletion-induced dendritic spine loss. Cereb Cortex 20:2423-2432.

Gerfen CR (1984) The neostriatal mosaic: compartmentalization of corticostriatal input and striatonigral output systems. Nature 311:461-464.

Gerfen CR (2006) Indirect-pathway neurons lose their spines in Parkinson disease. Nat Neurosci 9:157-158.

Gerfen CR, Surmeier DJ (2011) Modulation of striatal projection systems by dopamine. Annu Rev Neurosci 34:441-466.

Gerfen CR, Baimbridge KG, Miller JJ (1985) The neostriatal mosaic: compartmental distribution of calcium-binding protein and parvalbumin in the basal ganglia of the rat and monkey. Proc Natl Acad Sci U S A 82:8780-8784.

Gittis AH, Kreitzer AC (2012) Striatal microcircuitry and movement disorders. Trends Neurosci 35:557-564.

Graybiel AM (1990) Neurotransmitters and neuromodulators in the basal ganglia. Trends Neurosci 13:244-254.
Imre G (2007) The preclinical properties of a novel group II metabotropic glutamate receptor agonist LY379268. CNS Drug Rev 13:444-464.
Ingham CA, Hood SH, Taggart P, Arbuthnott GW (1998) Plasticity of synapses in the rat neostriatum after unilateral lesion of the nigrostriatal dopaminergic pathway. J Neurosci 18:4732-4743.
Jia Y, Mo SJ, Feng QQ, Zhan ML, OuYang LS, Chen JC, Ma YX, Wu JJ, Lei WL (2014) EPO-dependent activation of PI3K/Akt/FoxO3a signalling mediates neuroprotection in in vitro and in vivo models of Parkinson's disease. J Mol Neurosci 53:117-124.
Jimenez-Shahed J (2016) A review of current and novel levodopa formulations for the treatment of Parkinson's disease. Ther Deliv 7:179-191.
Kawaguchi Y (1997) Neostriatal cell subtypes and their functional roles. Neurosci Res 27:1-8.
Kim W, Im MJ, Park CH, Lee CJ, Choi S, Yoon BJ (2013) Remodeling of the dendritic structure of the striatal medium spiny neurons accompanies behavioral recovery in a mouse model of Parkinson's disease. Neurosci Lett 557 Pt B:95-100.
Lovinger DM (2010) Neurotransmitter roles in synaptic modulation, plasticity and learning in the dorsal striatum. Neuropharmacology 58:951-961.
Müller SK, Bender A, Laub C, Högen T, Schlaudraff F, Liss B, Klopstock T, Elstner M (2013) Lewy body pathology is associated with mitochondrial DNA damage in Parkinson's disease. Neurobiol Aging 34:2231-2233.
Ma Y, Zhan M, OuYang L, Li Y, Chen S, Wu J, Chen J, Luo C, Lei W (2014) The effects of unilateral 6-OHDA lesion in medial forebrain bundle on the motor, cognitive dysfunctions and vulnerability of different striatal interneuron types in rats. Behav Brain Res 266:37-45.
Ma Y, Feng Q, Ma J, Feng Z, Zhan M, OuYang L, Mu S, Liu B, Jiang Z, Jia Y, Li Y, Lei W (2013) Melatonin ameliorates injury and specific responses of ischemic striatal neurons in rats. J Histochem Cytochem 61:591-605.
Macpherson T, Morita M, Hikida T (2014) Striatal direct and indirect pathways control decision-making behavior. Front Psychol 5:1301.
Mallet N, Ballion B, Le Moine C, Gonon F (2006) Cortical inputs and GABA interneurons imbalance projection neurons in the striatum of parkinsonian rats. J Neurosci 26:3875-3884.
McDonald AJ (1992) Projection neurons of the basolateral amygdala: a correlative Golgi and retrograde tract tracing study. Brain Res Bull 28:179-185.
Morley JF, Duda JE (2012) Parkinson's disease and the risk of cerebrovascular pathology. Mov Disord 27:1471-1472.
Mu S, Lin E, Liu B, Ma Y, OuYang L, Li Y, Chen S, Zhang J, Lei W (2014) Melatonin reduces projection neuronal injury induced by 3-nitropropionic acid in the rat striatum. Neurodegenerative Diseases 14:139-150.
Murray TK, Messenger MJ, Ward MA, Woodhouse S, Osborne DJ, Duty S, O'Neill MJ (2002) Evaluation of the mGluR2/3 agonist LY379268 in rodent models of Parkinson's disease. Pharmacol Biochem Behav 73:455-466.
Perier C, Bové J, Vila M (2011) Mitochondria and programmed cell death in Parkinson's disease: apoptosis and beyond. Antioxid Redox Signal 16:883-895.
Planert H, Szydlowski SN, Hjorth JJ, Grillner S, Silberberg G (2010) Dynamics of synaptic transmission between fast-spiking interneurons and striatal projection neurons of the direct and indirect pathways. The Journal of Neuroscience 30:3499-3507.
Ragsdale CW, Graybiel AM (1988) Fibers from the basolateral nucleus of the amygdala selectively innervate striosomes in the caudate nucleus of the cat. J Comp Neurol 269:506-522.
Reiner A, Perera M, Paullus R, Medina L (1998) Immunohistochemical localization of DARPP32 in striatal projection neurons and striatal interneurons in pigeons. J Chem Neuroanat 16:17-33.
Schoepp DD, Jane DE, Monn JA (1999) Pharmacological agents acting at subtypes of metabotropic glutamate receptors. Neuropharmacology 38:1431-1476.
Tozzi A, de Iure A, Di Filippo M, Tantucci M, Costa C, Borsini F, Ghiglieri V, Giampà C, Fusco FR, Picconi B, Calabresi P (2011) The distinct role of medium spiny neurons and cholinergic interneurons in the D_2/A_2A receptor interaction in the striatum: implications for Parkinson's disease. J Neurosci 31:1850-1862.
Wirdefeldt K, Adami H-O, Cole P, Trichopoulos D, Mandel J (2011) Epidemiology and etiology of Parkinson's disease: a review of the evidence. Eur J Epidemiol 26 Suppl 1:S1-58.
Wood LD (2010) Clinical review and treatment of select adverse effects of dopamine receptor agonists in Parkinson's disease. Drug Aging 27:295-310.
Xiao D (2015) Acupuncture for Parkinson's disease: a review of clinical, animal, and functional magnetic resonance imaging studies. J Tradit Chin Med 35:709-717.
Zhou L, Wang ZY, Lian H, Song HY, Zhang YM, Zhang XL, Fan RF, Zheng LF, Zhu JX (2014) Altered expression of dopamine receptors in cholinergic motoneurons of the hypoglossal nucleus in a 6-OHDA-induced Parkinson's disease rat model. Biochem Biophys Res Commun 452:560-566.

Copyedited by James R, Haase R, Yu J, Li CH, Qiu Y, Song LP, Zhao M